ELSEVIER

Journal of Alloys and Compounds 434–435 (2007) 367–370

Journal of ALLOYS AND COMPOUNDS

www.elsevier.com/locate/jallcom

Study on the solid-phase sintering of the nano-structured heavy tungsten alloy powder

J.S.C. Jang [a,*], J.C. Fwu [a], L.J. Chang [a], G.J. Chen [a], C.T. Hsu [b]

[a] *Department of Materials Science and Engineering, I-Shou University, Kaohsiung, Taiwan, ROC*
[b] *Metal Industries Research and Development Center, Kaohsiung, Taiwan, ROC*

Available online 2 October 2006

Abstract

Recently, the high performance W–Ni–Fe–Co heavy tungsten alloy has become as the major core material of armor piercing ammunition. Since the melting temperature of tungsten element is too high to be fabricated by the melting process, that the W–Ni–Fe–Co alloy only can be synthesized by powder metallurgy process. In this study, two compositions of alloy powders, 93W–3Ni–2Fe–2Co and 93W–3.5Ni–1.5Fe–2Co, were selected for investigating their microstructure and mechanical properties after solid-phase sintering. These pre-alloyed powders with crystal cell size about 16 nm were synthesized by mechanical alloying (MA) the mixture of appropriate composition of pure elements in the Spex mill for 8 h. Then, the MA powders were compressed by cold isostatic pressing (CIP) and vacuum sintered at various temperature below 1400 °C for different time. Microstructure characterization of the sintered tungsten heavy alloys was conducted by means of SEM with EDS capability, X-ray diffraction (XRD), and TEM techniques. The result reveals that the microstructure of these sintered alloys was found to consist of the tungsten matrix phase and the Fe–Ni solid solution phase. The hardness of these sintered tungsten heavy alloy presents a trend with increasing sintering temperature and sintering time.

Keywords: Heavy tungsten alloy; Mechanical alloying; Solid-phase sintering

1. Introduction

Nowadays, the tungsten heavy alloys which tungsten content of 90–97 wt% [1,2] is applied to substitute uranium-depleted metals [3] as the core material of kinetic-energy penetrator [4]. Tungsten heavy alloys used to suffer from a use limit due to its blunt behavior while penetrating the tough target material [5]. The blunt behavior of tungsten alloy core is induced by the adiabatic shear deformation, which is related to a high strain rate and local shear deformation [6,7]. By refining the microstructure [8,9], we can improve the mechanical property of tungsten alloy core and so as to mend the blunt behavior. Since the mechanical alloying (MA) process has been proved as an effective method to refine many kinds of alloys, such as oxide dispersed strengthened alloy (ODS alloy) [10] and tungsten alloy [11]. Therefore, we endeavor to synthesize nano-structured heavy tungsten alloy powders by MA process for fabricating the bulk sample by solid-phase sintering. Their microstructure and mechanical properties after solid-phase sintering were examined by means of X-ray diffraction, scanning electron microscopy, and transmission electron microscopy.

2. Experimental

Heavy tungsten alloy powders with composition of 93W–3.0Ni–2.0Fe–2.0Co and 93W–3.5Ni–1.5Fe–2.0Co in at% were prepared by mechanical alloying (MA) the appropriate powder mixture of tungsten (2 μm), nickel (70 μm), iron (40 μm) and cobalt (35 μm) in a Spex mill, respectively. For avoiding the oxidation during powder milling, the mechanical alloying process was conducted under an Ar atmosphere for 8 h and the ball to powder weight ratio was kept at 5:1 by weight. The mechanically alloyed powders were then compressed into green compacts and vacuum sintered at 1250, 1300, 1350 and 1400 °C for 0.5 and 1 h, respectively. The microstructure evolution of the MA powder and the sintered bulk alloys of each sintering process were examined by X-ray diffractometry with Cu Kα wavelength, scanning electron microscopy (SEM) with electron dispersive spectrometry (EDS) capability, and transmission electron microscopy (TEM) techniques. Hardness of the sintered specimens was measured by using Akashi MVK-G1500 micro hardness tester.

3. Results and discussion

After 8 h milling by Spex Mill, the particle size of the alloy powder reached a uniform stable state with an average dimension about 3 μm, as shown in Fig. 1(a) and (b). The

* Corresponding author.
E-mail address: scjang@isu.edu.tw (J.S.C. Jang).

0925-8388/$ – see front matter © 2006 Elsevier B.V. All rights reserved.
doi:10.1016/j.jallcom.2006.08.215

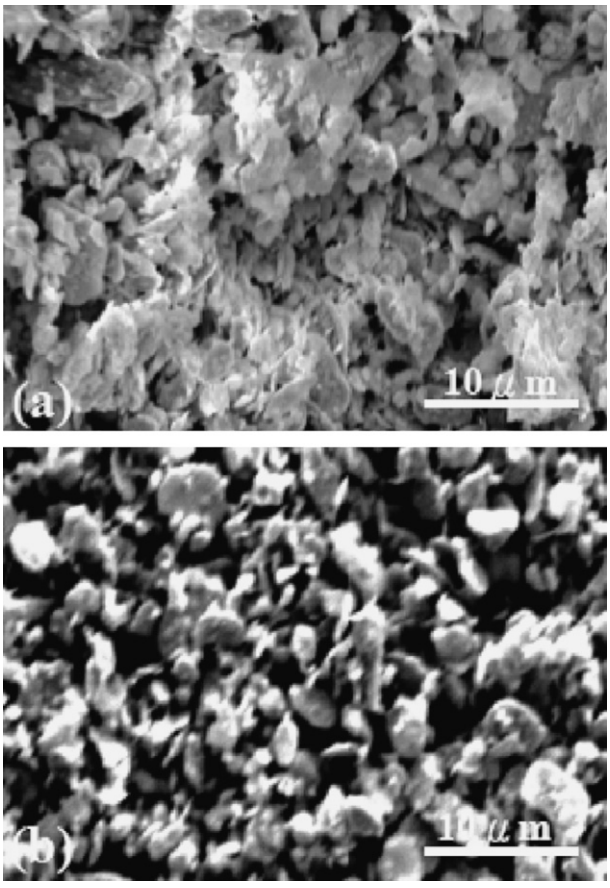

Fig. 1. The secondary electron images of tungsten heavy alloys after 8 h milling by Spex mill: (a) 93W–3.0Ni–2.0Fe–2.0Co alloy powder and (b) 93W–3.5Ni–1.5Fe–2.0Co alloy powder.

crystallite size of the MA 93W–3.5Ni–1.5Fe–2.0Co and MA 93W–3.0Ni–2.0Fe–2.0Co alloys powder which calculated by the Scherrer formula, $d = 0.9\lambda/\beta\cos\theta$, as a function of milling time is shown as Fig. 2. Where d is crystallite size, λ the X-ray wavelength, β the line width at one-half the maximum intensity, and θ the scattering angle. The apparent crystallite size of

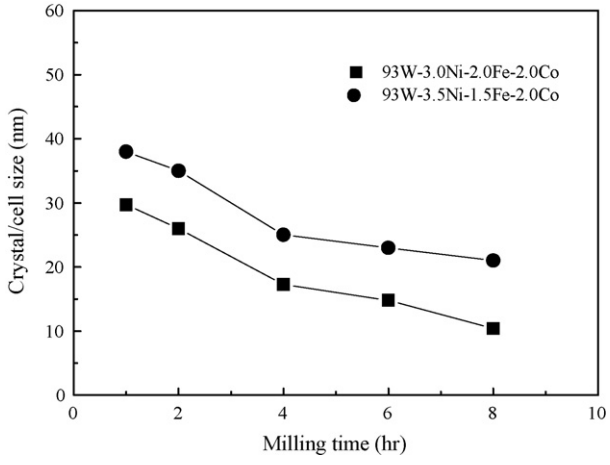

Fig. 2. The crystal size calculated by Scherrer formula as a function of milling time for tungsten heavy alloys: ■, 93W–3.0Ni–2.0Fe–2.0Co alloy; ●, 93W–3.5Ni–1.5Fe–2.0Co alloy.

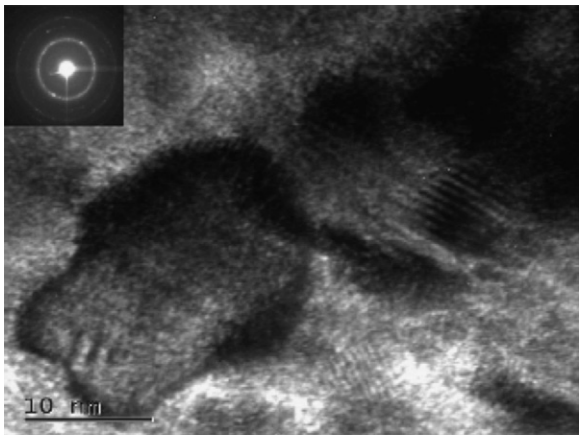

Fig. 3. TEM bright field images of the 93W–3.5Ni–1.5Fe–2.0Co alloy powder after 8 h milling by Spex mill.

these two MA alloys can reach to the nano-scaled dimension (less than 30 nm). This agrees closely with measuring by TEM observation (the average equiaxed cell or grain structure of the MA 93W–3.5Ni–1.5Fe–2.0Co alloy powder after 8 h milling is about 16 nm) as illustrated in Fig. 3.

The X-ray diffraction measurements on the 93W–3.5Ni–1.5Fe–2.0Co alloy sintered at different temperature below 1400 °C for 0.5 and 1 h, respectively revealed that only one set of main peaks belongs to bcc-structured tungsten phase (which is in very good agreement with the data of JCPDS file No.04-0806), as shown in Fig. 4. However, two relatively weak peaks which corresponding to Ni–Fe solid solution phase were also found in these diffraction patterns (which is in good agreement with the data of JCPDS file No.03-1206). In parallel, the relative intensity of the Ni–Fe solid solution phase seems increasing with sintering temperature.

SEM micrographs of Fig. 5(a)–(d) show the almost porous-free metallograph for each as-sintered 93W–3.5Ni–1.5Fe–2.0Co alloy at different temperature for 1 h, respectively. These SEM images all present two different phase area, the randomly

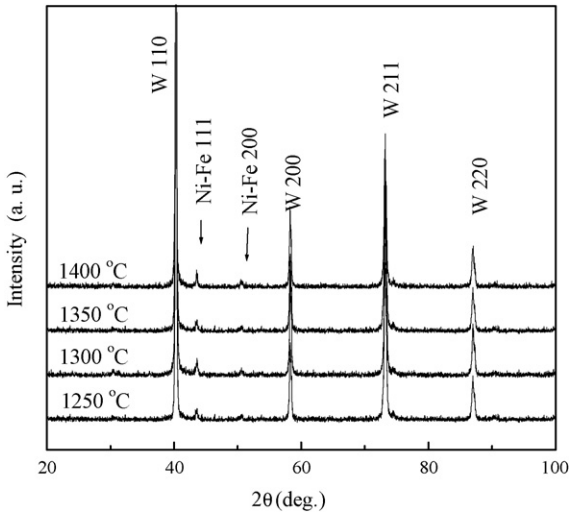

Fig. 4. X-ray diffraction patterns of the 93W–3.5Ni–1.5Fe–2.0Co alloy sintered at different temperature for 1 h.

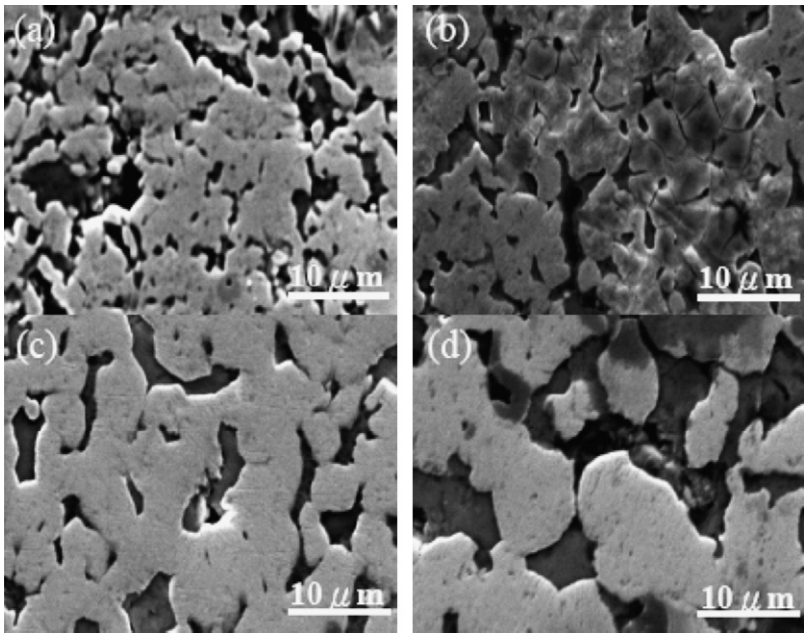

Fig. 5. The secondary electron images of the as-sintered 93W–3.5Ni–1.5Fe–2.0Co at (a) 1250 °C/1 h, (b) 1300 °C/1 h, (c) 1350 °C/1 h, and (d) 1400 °C/1 h.

distributed dark area phase surrounding the matrix phase (white area). According to the result of EDS analysis for the as-sintered 93W–3.5Ni–1.5Fe–2.0Co alloy, the matrix phase contains more than 96 at% of W which corresponding to the tungsten solid solution phase. On contrary, an extremely high Fe content (more than 42 at%) was examined at the dark area. With relating to the result of X-ray diffraction, the Fe–Ni solid solution phase is suggested to form at the dark area. The domain size of the matrix phase exhibit an increasing trend with sintering temperature and reaches to an average size about 8 μm for the alloy sintered at 1400 °C for 1 h. This indicates that the higher sintering temperature, the more intensity of the thermal vibration and frequency to increase the rate of vacancy motion and so as to enhance the grain growth of the tungsten rich phase at higher sintering temperature. On contrary, the microstructure of the 93W–3.5Ni–1.5Fe–2.0Co alloy after liquid-phase sintering (sintered at the temperature above 1500 °C for 1 h) exhibits much larger domain size (15 μm) and more retained porosity (about 7.5 vol.%) than the solid-phase sintered alloy (1400 °C, 1 h) [12] as shown in Fig. 6. TEM dark-field image of the 93W–3.5Ni–1.5Fe–2.0Co alloy after sintered at 1400 °C for 1 h reveals that many nano tungsten solid solution phase embedded beside the tungsten matrix phase as shown in the Fig. 7. The composition of these nano particles were found to have much higher Ni (∼9 at%) and Fe (∼4 at%) content than that (Ni: 1.9 at% and Fe: 1.8 at%)in the tungsten matrix phase by EDS analysis.

The hardness as a function of sintering time at different temperature for 93W–3.0Ni–2.0Fe–2.0Co and 93W–3.5Ni–1.5Fe–2.0Co alloys is shown as Fig. 8. With increasing the temperature and the time of sintering would simultaneously increases the hardness significantly for these two alloys. The

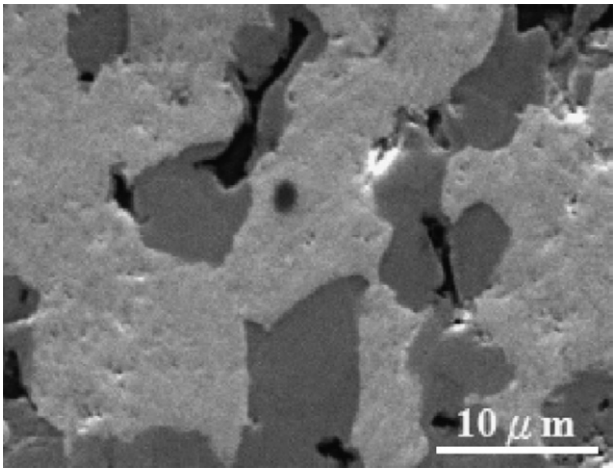

Fig. 6. The secondary electron images of 93W–3.5Ni–1.5Fe–2.0Co alloy after liquid-phase sintering (sintered at the temperature above 1500 °C for 1 h).

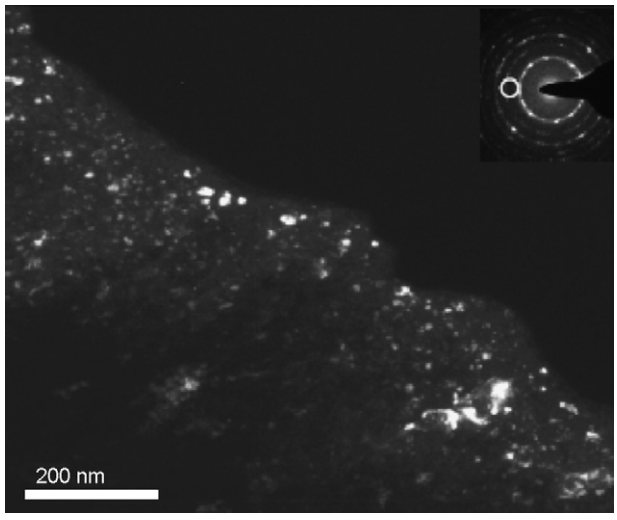

Fig. 7. TEM dark-field image of Ni–Fe (1 1 1) for the 93W–3.5Ni–1.5Fe–2.0Co alloy after sintered at 1400 °C for 1 h.

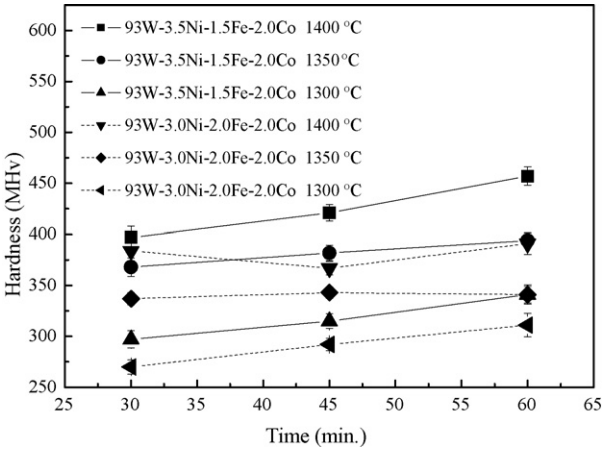

Fig. 8. Hardness as functions of sintering time at the different temperature below 1400 °C.

maximum hardness can be reached up to Hv 450 ± 20 for the 93W–3.5Ni–1.5Fe–2.0Co alloy sintered at 1400 °C for 1 h. This presents 30% increase in hardness in comparison with the same alloy sintered at 1250 for 1 h, Hv 360 ± 30. In addition, the dark area phase which containing nano tungsten solid solution phase (Hv 540 ± 30) exhibits much higher hardness than that of the W matrix (Hv 420 ± 20). Therefore, the increase of hardness for the sample sintered at higher temperature is suggested contributing by the formation of nano tungsten solid solution phase as well as the increase of densification for the alloy sample.

4. Conclusion

The solid phase sintered 93W–3.0Ni–2.0Fe–2.0Co and 93W–3.5Ni–1.5Fe–2.0Co alloy by using nano-structured MA powders was characterized by X-ray diffraction, SEM, EDS, and TEM techniques. The result can be summarized as follow:

(1) X-ray diffraction revealed that the bcc soild solution tungsten phase, the Fe_7W_6 intermetallic phase, and the Fe–Ni solid solution phase formed after 1 h sintering at 1250, 1300, 1350, and 1400 °C, respectively.
(2) The domain size of the matrix phase for the 93W–3.5Ni–1.5Fe–2.0Co alloy exhibit an increasing trend with sintering temperature and reaches to an average size about 8 μm for the alloy sintered at 1400 °C for 1 h. On contrary, the microstructure of the 93W–3.5Ni–1.5Fe–2.0Co alloy after liquid phase sintering (sintered at the temperature above 1500 °C for 1 h) exhibits much large domain size (15 μm) and more retained porosity (about 7.5 vol.%) than the solid phase sintered alloy (1400 °C, 1 h).
(3) TEM observation revealed that many nano tungsten solid solution phase embedded beside the tungsten matrix phase for the 93W–3.5Ni–1.5Fe–2.0Co alloy after sintered at 1400 °C for 1 h. The composition of these nano particles were found to have much higher Ni (∼9 at%) and Fe (∼4 at%) content than that (Ni: 1.9 at% and Fe: 1.8 at%) in the tungsten matrix phase by EDS analysis.
(4) The hardness of 93W–3.0Ni–2.0Fe–2.0Co and 93W–3.5Ni–1.5Fe–2.0Co alloys shows an increasing trend with sintering temperature and time simultaneously. The maximum hardness can be reached up to Hv 450 ± 20 for the 93W–3.5Ni–1.5Fe–2.0Co alloy sintered at 1400 °C for 1 h. Additionally, the dark area phase which containing Fe_7W_6 intermetallic phase (Hv 540 ± 30) exhibits much higher hardness than that of the W matrix (Hv 320 ± 20). Therefore, the increase of hardness for the higher temperature sintered sample is suggested contributing by the formation of nano tungsten solid solution phase as well as the increase of densification for the alloy sample.

Acknowledgements

The authors would like to gratefully acknowledge the sponsorship from the National Science Council of R.O.C. under the project NSC94-2623-7-214-001 and NSC94-2218-E-110-009.

References

[1] S.H. Hong, Ho.J. Ryu, W.H. Baek, Mater. Sci. Eng. A333 (2002) 187.
[2] T.W. Penrice, Metals Hand book, vol. 7, 9th ed., ASM Inter, 1984, 688.
[3] L.S. Magness, T.G. Farrand, Proceedings of Army Science Conference, Durham, 1990, p. 149.
[4] R.J. Dowding, M.C. Hogwood, L. Wong, R.L. Woodward, in: A. Bose, R.J. Dowding (Eds.), Proceedings of Second International Conference On Tungsten and Refractory Metals, New Jersey, 1994, p. 3.
[5] Z. He, T.H. Courtney, Mater. Sci. Eng. A315 (2001) 166.
[6] K.T. Ramesh, R.S. Coates, Met. Trans. A23 (1992) 2625.
[7] A. Bose, H.R.A. Cougue, J. Lang ford Int. J. Powder Met. 28 (1992) 383.
[8] D. Chaiat, E.Y. Gutmanas, I. Gotman, Proceedings of the Second International Conference On Tungsten and Refractory Metals, 1994, p. 57.
[9] W.E. Gurwell, in: A. Bose, R.J. Dowding (Eds.), Proceedings of the Second International Conference On Tungsten and Refractory Metals, New Jersey, 1994, p. 65.
[10] J.S. Benjamin, T.E. Volin, Metall. Trans. 5 (1974) 1929.
[11] S. Cytron, Proceedings of the International Conference Advanced Composite Materials, TMS, 1993, p. 973.
[12] C.T. Hsu, Study on the Processing and Properties of Solid-Phase Sintering in W–Ni–Fe–Co Tungsten Heavy Alloy, Master dissertation, Department of Materials Science and Engineering, I-Shou University, Kaohsiung, Taiwan, ROC, 2004, p. 134.